# Globular and Protofibrillar Aβ Aggregates Impair Neurotransmission by Different Mechanisms

**ARTICLE** *in* BIOCHEMISTRY · FEBRUARY 2013

Impact Factor: 3.02 · DOI: 10.1021/bi3016444 · Source: PubMed

BIOCHEMISTRY
including biophysical chemistry & molecular biology

Article

pubs.acs.org/biochemistry

# Globular and Protofibrillar Aβ Aggregates Impair Neurotransmission by Different Mechanisms

Jens Moreth,*[,†] Katja S. Kroker,[†] Daniel Schwanzar,[‡] Cathrin Schnack,[‡] Christine A. F. von Arnim,[‡] Bastian Hengerer,[†] Holger Rosenbrock,[†] and Lothar Kussmaul[†]

[†]Department of CNS Diseases Research Germany, Boehringer Ingelheim Pharma GmbH & Co. KG, Birkendorfer Strasse, Biberach an der Riss D-88397, Germany

[‡]Department of Experimental Neurology, University of Ulm, Helmholtz Strasse, Ulm D-89081, Germany

Supporting Information

**ABSTRACT:** In Alzheimer's disease, substantial evidence indicates the causative role of soluble amyloid β (Aβ) aggregates. Although a variety of Aβ assemblies have been described, the debate about their individual relevance is still ongoing. One critical issue hampering this debate is the use of different methods for the characterization of endogenous and synthetic peptide and their intrinsic limitations for distinguishing Aβ aggregates. Here, we used different protocols for the establishment of prefibrillar Aβ assemblies with varying morphologies and sizes and compared them in a head-to-head fashion. Aggregation was characterized via the monomeric peptide over time until spheroidal, protofibrillar, or fibrillar Aβ aggregates were predominant. It could be shown that a change in the ionic environment induced a structural rearrangement, which consequently confounds the delineation of a measured neurotoxicity toward a distinct Aβ assembly. Here, neuronal binding and hippocampal neurotransmission were found to be suitable to account for the synaptotoxicity to different Aβ assemblies, based on the stability of the applied Aβ aggregates in these settings. In contrast to monomeric or fibrillar Aβ, different prefibrillar Aβ aggregates targeted neurons and impaired hippocampal neurotransmission with nanomolar potency, albeit by different modalities. Spheroidal Aβ aggregates inhibited NMDAR-dependent long-term potentiation, as opposed to protofibrillar Aβ aggregates, which inhibited AMPAR-dominated basal neurotransmission. In addition, a provoked structural conversion of spheroidal to protofibrillar Aβ assemblies resulted in a time-dependent suppression of basal neurotransmission, indicative of a mechanistic switch in synaptic impairment. Thus, we emphasize the importance of addressing the metastability of *prefacto* characterized Aβ aggregates in assigning a biological effect.

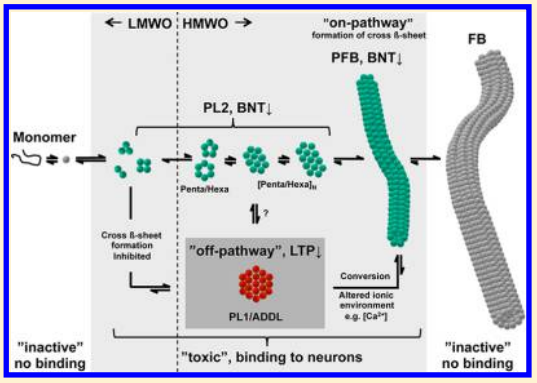


Despite the well-accepted pathogenic role of amyloid β (Aβ) in Alzheimer's disease,[1] the underlying pathogenic mechanism is still elusive.[2] Aβ is generated from amyloid precursor protein by sequential proteolysis.[3] This is followed by its self-association from monomeric to soluble prefibrillar Aβ, which further assembles into insoluble Aβ fibrils that deposit in the brain as amyloid plaques. Because the number of these plaques, as opposed to the presence of soluble Aβ-aggregates,[4] does not correlate well with the severity of dementia,[5] the amyloid hypothesis has been reformulated, positioning soluble Aβ aggregates as the prime toxic agent, causing synapse loss and decreased cognitive performance.[6] Substantial efforts have been made to identify the "most" toxic Aβ aggregate, derived from synthetic peptide and endogenous sources, i.e., cell culture, transgenic animals, and post mortem tissue. These studies resulted in the description of different soluble, prefibrillar Aβ species, which all show pathophysiological relevance, i.e., neurotoxicity and impaired neurotransmission.[7]

Although the parameters used predominantly for the differentiation of Aβ aggregates are size and molecular weight (MW), a direct comparison of these aggregates is difficult because this comparison is based on different methods.[7] Furthermore, some of these methods affect aggregation per se, e.g., the presence of SDS,[8,9] limiting the suitability of SDS–PAGE for characterization. Other methods such as atomic force microscopy (AFM) and transmission electron microscopy (TEM) are restricted to high protein concentrations and purities; however, these do offer structural information on a nanometer scale.[10,11]

Because of the difficulty in purifying endogenous Aβ species without interfering with the native state of the assemblies,[12] synthetic Aβ has been favored for biophysical characterization, using various Aβ peptides, as well as a range of solubilization and aggregation conditions[10,13−15] to generate Aβ aggregates of different sizes and morphologies.[7] Most of these Aβ species are temporally transient and metastable intermediates "on-path-

**Received:** December 9, 2012
**Revised:** January 28, 2013
**Published:** February 1, 2013

way" to fibrils (e.g., hexamer and protofibrils), but some [e.g., Aβ oligomers (AβO) or "Alzheimer-derived diffusible ligands" (ADDLs)] reach equilibrium, i.e., do not undergo a significant change over the time of observation in the respective aggregation buffer. These species are considered as "off-pathway" assemblies, indicative of a nonlinear process of aggregation.[16,17] In addition, several studies showed that a change in the molecular interactions induced by an altered environment (e.g., buffer, peptide concentration, and temperature) results in a rapid rearrangement of *prefacto*-characterized Aβ aggregates.[18,19] Thus, the metastability hampers the elucidation of aggregate structure and also the characterization of pathophysiological effects. Consequently, the stability of *prefacto*-characterized Aβ aggregates in the experimental paradigms should be evaluated cautiously before a pathogenic mechanism is attributed to a certain Aβ species. Although different soluble Aβ species have been proposed to mediate synaptotoxicity via different mechanisms and targets,[7,17,18,20,21] studies aiming for a head-to-head comparison of different prefibrillar Aβ aggregates are rarely found. Here, the morphology and MW of monomeric, spheroidal, protofibrillar, and fibrillar Aβ assemblies were characterized by AFM and dynamic (DLS) and static multiangle (MALS) light scattering, while minimizing interference on Aβ aggregation. Furthermore, pathophysiological effects were assessed under conditions where Aβ aggregate reorganization was minimized. Herein, neuronal interaction was found only for prefibrillar Aβ assemblies mediating impairment of neurotransmission by at least two independent pathways.

## EXPERIMENTAL PROCEDURES

**Aβ Preparations.** Aβ40 or Aβ42 (desalted peptide, Bachem) was dissolved in HFIP (Fluka) to a final concentration of 1 mM, sonified for 10 min, gently shaken for 1 h at room temperature, snap-frozen in liquid nitrogen, and lyophilized. The peptide was stored at −80 °C until it was used. If not stated otherwise, Aβ was solubilized at 1 mM in NaOH (10 mM), sonified for 2 min, and diluted to a final concentration of 100 μM in the respective aggregation buffer. After incubation, all preparations except fibrils were centrifuged (15000*g* for 10 min), and the supernatants were analyzed. For monomeric Aβ (Mono), solubilized Aβ40 was diluted in PBS, centrifuged, and used within 1 h. For prefibrillar Aβ aggregates (PL1 and PL2), solubilized Aβ42 was diluted in phenol red-free Ham's F12 (PL1; Invitrogen) or DMEM (PL2; Invitrogen) and incubated at 4 °C for 20 h. For protofibrils (PFB), solubilized Aβ42 was diluted in PBS and incubated at 4 °C for 20 h. For fibrils (FB), solubilized Aβ42 was diluted in 10 mM HCl and incubated at 37 °C for 20 h.

**DLS.** Cumulative fitting was used to measure the global hydrodynamic radius ($R_{H,c}$) of the aggregate solution, until pseudoequilibrium was reached. The regularization method was used to determine the size distribution of Aβ aggregates ($R_{H,r}$[22]).

**AF4-MALS.** AF4 separates molecules by differences in Brownian motion, without a stationary phase, minimizing sheer forces and protein−matrix interactions.[23,24] The AF4 system (Eclipse III+, Wyatt Technology) was controlled by an high-performance liquid chromatography system (Agilent, 1200 series), defining sample loading (10−50 μg/injection) and flow conditions. AF4 was optimized to separate particles with a molecular weight of 4−2000 kDa using a 1 kDa cutoff PES membrane, a 480 μm spacer, PBS as the eluent, and the following flow conditions: detector flow, 1 mL/min; cross-flow, 3 mL/min from 0 to 10 min, 3.0 to 0.1 mL/min from 10 to 15 min, and 0.1 mL/min from 15 to 30 min. Fractions were analyzed by $UV_{220}/UV_{280}$ and MALS (DAWN Heleos, Wyatt Technology). Data from MALS were analyzed by ASTRA (Wyatt Technology).

**AFM.** Measurements were performed with a NanoScope IIIa (Veeco) in tapping mode, using RTESP-SS tips (Veeco) and muscovite Mica. The scanning area was set to 2 μm × 2 μm at ≤2 Hz. Captured data were processed with SPIP (Image Metrology). Thirty microliters of the Aβ preparation (10 μM) was added for 2 min at room temperature, rinsed with 2 mL of Milli-Q-water, and dried immediately with nitrogen for 2 min. The spatial tilt of raw images was fit by a polynomial fit (third-order) and line-wise correction. Particle recognition using the watershed algorithm[25] was validated with standardized gold particles 2, 5.5, and 14.5 nm in diameter (Ted Pella Inc.). Lateral dimensions were used as relative measures only according to tip size broadening. The watershed algorithm (optimized for spheroidal structures) was not suitable for particle recognition of fibrils, because of oversegmentation (i.e., underestimation of length). Therefore, FB was analyzed using the threshold algorithm.

**Primary Neuronal Culture.** Procedures involving animals (Janvier, Le Genest Saint Isle, France) and their care were conducted in a manner consistent with institutional and European Union guidelines (EEC Council Directive 86/609) and were approved by the Ethical Committee of the respective regional councils. Hippocampal neurons derived from C57BL6 mice were prepared as previously described by Brewer et al.[26]

**Neurotoxicity.** Neuronal cultures (DIV21) were treated with Aβ aggregates (3 μM) prediluted in neurobasal medium and incubated for 48 h. The viability of cells was assessed by MTT assay according to the manual (Invitrogen).

Binding of neuronal Aβ to matured hippocampal neurons (DIV21) was assessed by a modified protocol of Lacor et al.,[27] using biotinylated Aβ aggregates, detected by streptavidin-AF488 (1 μg/mL; Invitrogen). Neurons were stained with anti-CaMK (1 μg/mL; Enzo Life Science) using the IR-700 anti-mouse secondary antibody (0.1 μg/mL; Licor Odyssey).

**Electrophysiology.** Male Wistar rats (7 weeks old) were sacrificed by decapitation. The preparation of brain slices and recording of LTP were conducted according to the method of Kroker et al.[28] Briefly, transverse hippocampal slices (400 μm) were prepared and allowed to recover at room temperature in aCSF. After equilibration for at least 30 min, field excitatory postsynaptic potentials (fEPSPs) were elicited in the CA1 region by stimulation of the Schaffer collateral-commissural fibers in the *stratum radiatum*. The amplitudes of fEPSPs were used as the parameter of interest.[29] NMDA receptor (NMDAR)-dependent LTP was induced by high-frequency stimulation (HFS; 100 Hz, 1s[28]).

**Presentation of Data and Statistical Analysis.** All results were reproduced at least three times in independent experiments. If not stated otherwise, data represent mean values ± the standard deviation of *n* experiments. Comparison of groups was analyzed by an unpaired *t* test or one-way ANOVA followed by Bonferroni's post hoc test, using Prism (GraphPad version 5.04). $p < 0.05$ was considered statistically significant. The significance level is indicated as follows: $*p < 0.05$, $**p < 0.01$, and $***p < 0.001$. n.s. indicates nonsignificant differences.

Further methodological details are given in the Supporting Information.

## RESULTS

**Characterization of Different Aβ Assemblies.** The initial solubilization of the Aβ peptide is a crucial step in establishing robust and reproducible Aβ preparations. Therefore, we compared different solvents for solubilization and analyzed the morphology and size of the resulting Aβ aggregates. We confirmed that solubilization in hexafluoro-2-propanol (HFIP) and NaOH was superior to that in DMSO for the initiation of Aβ aggregation from the monomeric state, based on the generation of monodisperse Aβ solutions as assessed by DLS. Aβ solubilized in DMSO revealed polydisperse solutions with an $R_H$ of >3 nm. Aβ42 in NaOH or HFIP showed a hydrodynamic radius ($R_H$) of 1.8 nm, which increased with the time of incubation in contrast to Aβ40 showing a stable $R_H$ of monomeric Aβ [1.1−1.3 nm (Figure S2C of the Supporting Information and Table 1A)].

The subsequent dilution of NaOH-solubilized Aβ in different buffers induced aggregation and resulted in pseudostable aggregates (Figure S2D of the Supporting Information) with different morphology and size distributions (Figure 1), which we define as monomeric (Mono), oligomeric (PL1 and PL2), protofibrillar (PFB), and fibrillar (FB) preparations. Aβ42 instantaneously aggregated in all buffers that were investigated, thus precluding its use as a monomeric preparation. In contrast, Aβ40 revealed a constant $R_H$ in line with monomeric Aβ [Mono (Figure S2D of the Supporting Information)]. The established preparations revealed conformational differences (Figure S5 of the Supporting Information). ThioT fluorescence did not increase for Mono and PL1 but did significantly for PFB and FB, indicating the generation of cross β-sheet, which was confirmed by the appearance of curvilinear structures in TEM. A11 dot blots of PL1 and PL2 resulted in strong A11 immunoreactivity, and Mono, PFB, and FB are A11-negative.

Further characterization of the individual Aβ preparations was performed by AFM followed by semiautomated particle recognition, upon validation with standardized gold colloids (Figure S1 of the Supporting Information) to assess the morphology (height and length) of the formed Aβ aggregates. The MW distribution of these preparations was determined by asymmetrical flow field-flow fractionation (AF4) followed by MALS (Figure 1 and Table 1B). For the determination of MW, we considered AF4-MALS superior to classical size-exclusion chromatography and electrophoresis based on a stable ionic environment and fast separation without the need of a stationary matrix. The combination of AFM, DLS, and AF4-MALS allowed a precise characterization of the morphology, size, and MW with minimized interference with the delicate equilibrium of the Aβ aggregate distributions in the respective preparations. Herein, Mono appeared as unstructured particles with a monodisperse height of 1.1 ± 0.4 nm and a corresponding MW of 4.5 kDa at peak (85%). PL1 appeared as spheroidal particles with a monodisperse height distribution of 6.4 ± 3.1 nm with <20 kDa aggregates (23%), the predominant peak at 73 kDa (46%), and the remaining 21% larger than 100 kDa. PL2 exhibited a height of 2.4 ± 2.1 nm; however, heterogeneity was indicated by two maxima (P1 and P2) at 1.5 nm (PL2-P1, 75%) and 5.6 nm (PL2-P2, 25%), with the latter being elongated (40 nm) compared to PL1 and PL2-P1 (both 20 nm). In AF4-MALS, PL2 showed peaks at 6 kDa (33%) and 60 kDa (42%), with 25% larger than 100 kDa. PFB showed elongated particles (78 nm) with a height of 5.3 ± 1.0 nm, comparable to PL1 and PL2-P2, and a trimodal distribution in AF4-MALS, with maxima at 6 kDa (10%), a shoulder at 60 kDa (23%), and a second peak at 644 kDa (67%). FB exhibited fibrillar assemblies with a height of ∼6 nm and a length of >1 μm obtained by manual segmentation. The particle recognition analysis in AFM and MW determination by AF4-MALS was not suitable because of oversegmentation (Figure S3 of the Supporting Information) and inversed elution, respectively.[24] In summary, our setup revealed continuous MW distributions for all Aβ preparations and no single molecular entity. These preparations were stable in their individual environment and varied significantly from each other with regard to conformation, predominant size, morphology, and MW.

**Aβ Aggregates Are Metastable.** Because ab initio Aβ aggregation can be affected by the selected ionic environment,[10] we characterized the stability in DLS kinetics of *prefacto*-characterized Aβ aggregates under the conditions applied to assess their bioactivity, i.e., neurotoxicity (Figure 2), neuronal binding, and neurotransmission (Figure 3 and Figure S6 of the Supporting Information). In DLS, the $R_H$ has been analyzed by

**Table 1**

| Solubilization of Aβ in Different Solvents[a] | | | | |
|---|---|---|---|---|
| protein | MW (kDa) | $R_{H,r}$ (nm) | $R_{H,calc}$ (nm) | $n_{exp}$ |
| aprotinin | 6.5 | 1.7 ± 0.2 | 1.6 | 5 |
| BSA | 66 | 3.3 ± 0.2 | 3.5 | 5 |
| thyroglobulin | 669 | 10.1 ± 0.3 | 10.1 | 5 |
| Aβ40-HFIP | 4.5 | 1.5 ± 0.4 | 1.3 | 3 |
| Aβ42-HFIP | 4.5 | 1.3 ± 0.6 | 1.3 | 3 |
| Aβ40-NaOH | 4.5 | 1.5 ± 0.4 | 1.3 | 3 |
| Aβ42-NaOH | 4.5 | 1.8 ± 0.4 | 1.3 | 3 |
| Aβ40-DMSO | | | | |
| P1 (35%) | 4.5 | 2−10 | 1.3 | 3 |
| P2 (65%) | 4.5 | >150 | 1.3 | 3 |
| Aβ42-DMSO | | | | |
| P1 (40%) | 4.5 | 2−10 | 1.3 | 3 |
| P2 (60%) | 4.5 | >500 | 1.3 | 3 |
| Particle Analysis of Aβ Preparations in AFM[b] | | | | |
| Aβ preparation | height (nm) | length (nm) | $N$ | $n_{exp}$ |
| CTL (no Aβ) | 0.2 ± 0.1 | 71.3 ± 57.6 | 1186 | 5 |
| Mono | 1.1 ± 0.4 | 11.0 ± 6.6 | 5789 | 10 |
| PL1 | 6.4 ± 3.1 | 24.1 ± 6.9 | 5162 | 10 |
| PL2 Average | 2.4 ± 2.21 | 20.3 ± 15.1 | 2168 | 5 |
| P1 | 1.5 ± 0.6 | 20.5 ± 14.8 | 1627 | 5 |
| P2 | 5.6 ± 1.7 | 37.6 ± 16.3 | 541 | 5 |
| PFB | 5.3 ± 1.0 | 78.1 ± 61.8 | 5053 | 10 |
| FB | 6.2 ± 1.5 | 211.8 ± 335.2 | 710 | 10 |

[a]Measured $R_{H,r}$ (DLS) and calculated $R_H$ ($R_{H,calc}$) of standard proteins (0.5 mg/mL in PBS) and Aβ peptides (0.5 mg/mL) in different solvents. $R_{H,calc}$ was calculated on the basis of MW with Dynamics (Wyatt Technology). Measured and calculated $R_H$ values for standard proteins differed by <10%. For Aβ solubilization in NaOH or HFIP, $R_{H,r}$ did not differ significantly from $R_{H,calc}$. However, Aβ solubilized in DMSO revealed two populations (P1 and P2); in this instance, averaged values are shown. [b]Data represent means ± the standard deviation of $N$ particles, derived from $n$ independent experiments; all prefibrillar preparations as well as Mono and blank mica differed significantly from each other in height and length (***$p < 0.001$), with the exception of PL1 and PL2 (no significant difference in length). PL2 is depicted as average and as populations 1 and 2 (P1 and P2, respectively) based on the observed bimodal distribution. FB was not included in this statistical analysis because of the different particle recognition algorithm.


dx.doi.org/10.1021/bi3016444 | Biochemistry 2013, 52, 1466−1476

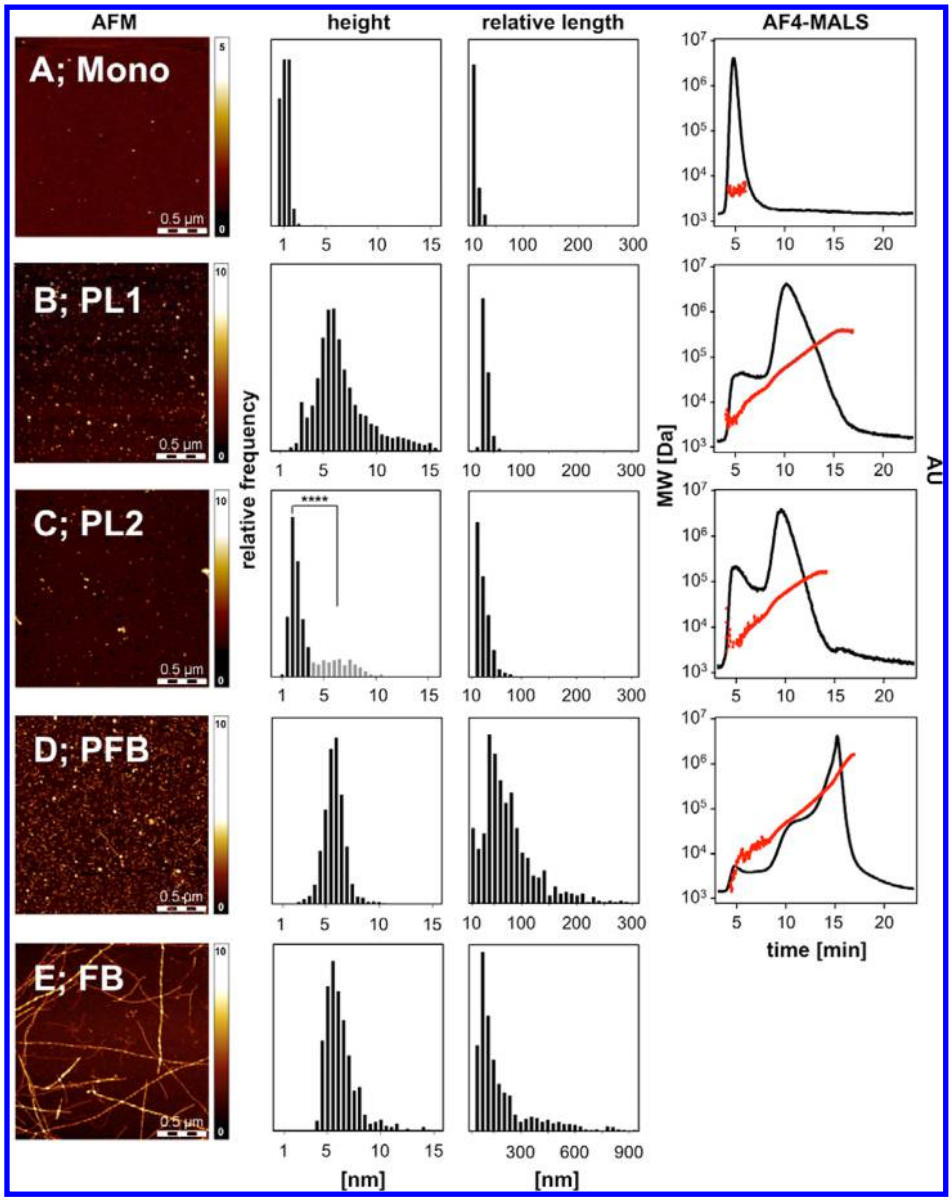


**Figure 1.** Distribution of height, apparent length, and MW determined by AFM-SPIP and AF4-MALS for A$\beta$ monomer (A), PL1 (B), PL2 (C), PFB (D), and FB (E). Via AFM, PL2 revealed a bimodal height distribution, which was further distinguished in PL2-P1 (<3 nm) and PL2-P2 (>3 nm). P1 and P2 differed significantly in height and length ($p < 0.0001$). Data represent cumulative distributions of at least five individual experiments for each preparation. AFM images have dimensions of 2 $\mu$m × 2 $\mu$m. The obtained height and relative length are listed in Table 1. Via AF4-MALS, the mass distribution (black) and MW (red) of A$\beta$ preparations were obtained.

a cumulative ($R_{H,c}$) and a regularized fit ($R_{H,r}$) to determine a global change in size and the size distribution of A$\beta$ aggregates, respectively. Centrifugation and dilution in the respective aggregation buffer (binding experiments) did not change $R_{H,c}$ or $R_{H,r}$ as exemplified for PL1 6 h postdilution (Figure 2A). However, dilution of PL1 in artificial cerebrospinal fluid (aCSF, neurotransmission experiments) induced aggregate reorganization, shown by an increase in $R_{H,c}$ and the occurrence of large aggregates after 1 h [$PL1_{aged}$ (Figure 2B)] and the appearance of protofibrillar and fibrillar aggregates in AFM (Figure 2D,E). Similarly, dilution of Mono in NB medium (neurotoxicity experiments) increased $R_{H,c}$, indicative of the generation of large aggregates, confirmed by 40% insoluble A$\beta$ recovered in the pellet after 48 h (Figure 2G). A critical factor, sufficient to induce reorganization of preformed A$\beta$ aggregates, was the $Ca^{2+}$ concentration, which was low in the buffers used for Mono and PL1 (0 and 0.3 mM, respectively) but high in NB medium (1.8 mM) and aCSF (2 mM). Dilution of PL1 in high-$Ca^{2+}$ concentration Ham's F12 (2 mM) was sufficient to induce reorganization of PL1 (Figure 2C) as it was observed for dilution of PL1 in aCSF. In summary, subtle changes in the ionic environment were sufficient to induce rapid reorganization of A$\beta$ aggregates.

**Bioactivity of Different A$\beta$ Aggregates.** MTT toxicity, differential neuronal binding, and hippocampal neurotransmission have been applied to test whether different A$\beta$ aggregates also reveal different neuronal impairment or toxicity. Modest but significant neurotoxicity was observed for all A$\beta$ preparations when compared to buffer controls, but not between individual A$\beta$ preparations (Figure 2F). The lack of aggregate stability over 48 h underlines the limitations of the MTT toxicity experiment for attributing a neurotoxic effect to a


dx.doi.org/10.1021/bi3016444 | *Biochemistry* 2013, 52, 1466−1476

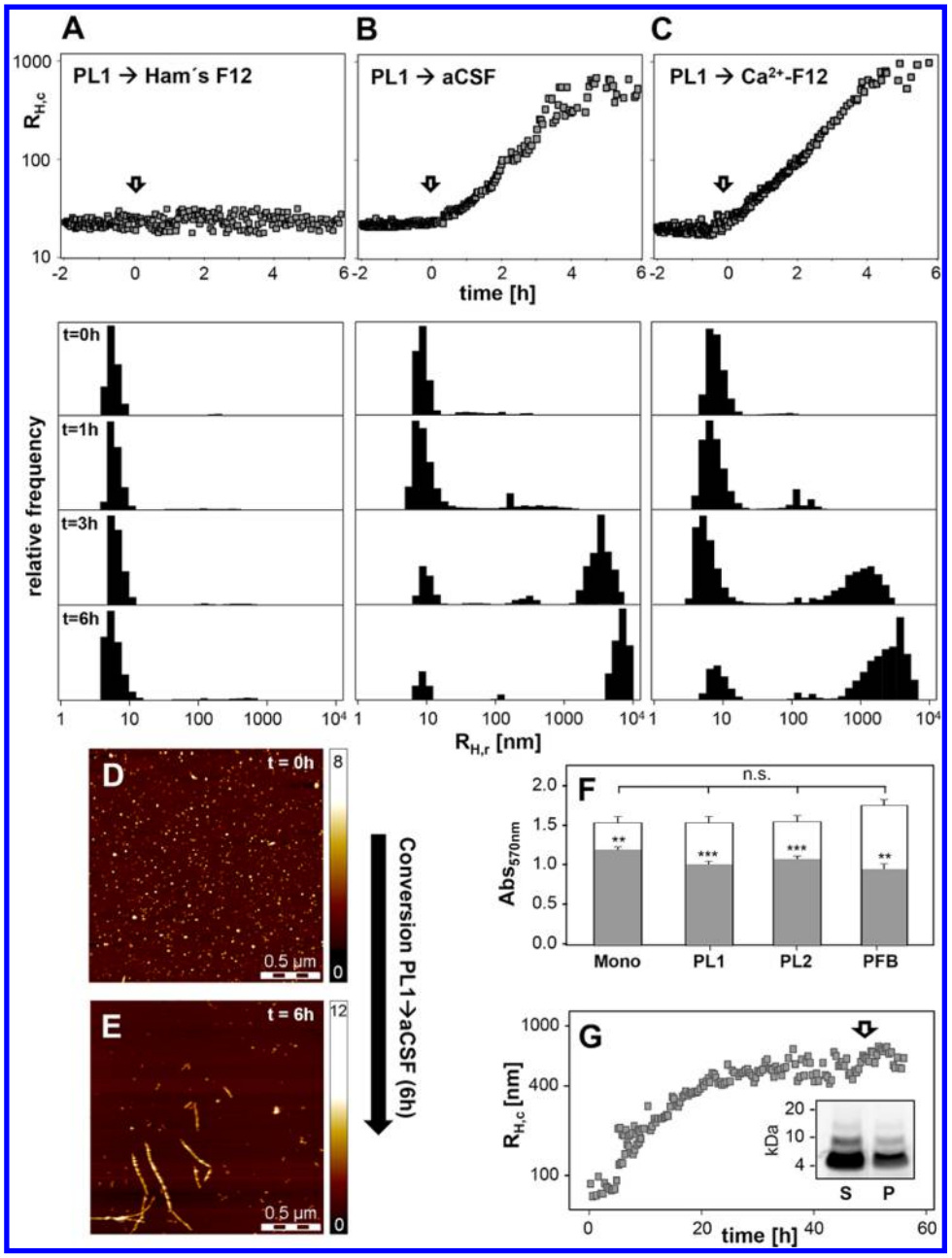


**Figure 2.** Metastability of A$\beta$ aggregates. Dilution of PL1 in aCSF (1:3) and incubation for 6 h (room temperature) resulted in conversion to protofibrillar and fibrillar aggregates as shown by AFM (D and E). (A–C) Stability of PL1 after centrifugation ($t$ = −2 h) and dilution ($t$ = 0 h) in Ham's F12 (A), aCSF (B), and high-$Ca^{2+}$ concentration F12 (C). PL1 (100 $\mu$M) was centrifuged (10 min at 20000$g$) and measured in DLS for 2 h (−2 to 0 h), followed by dilution in the respective medium (1:3, arrow), and measured for an additional 6 h. $R_{H,r}$ distributions (bottom panels of A–C) were determined at the indicated time points. Dilution of OL2 in aCSF or high-$Ca^{2+}$ concentration F12 caused a time-dependent increase in $R_{H,r}$, whereas dilution in Ham's F12 did not induce a change in $R_{H,r}$. Large aggregates ($R_H$ > 100 nm) became predominant after 3 h in panels B and C. (F) Neurotoxicity of A$\beta$ aggregates on primary hippocampal neurons revealed modest neurotoxicity of A$\beta$ (3 $\mu$M; 55–78% viability, ***$p$ < 0.001) compared to aggregation buffer without A$\beta$ (white bars). (G) DLS kinetics of Mono upon dilution in NB medium. The inset shows centrifugation of the diluted monomeric preparation after 48 h (arrow; 15000$g$ for 10 min) followed by 6E10-WB indicated for insoluble aggregates (S, supernatant; P pellet).

certain A$\beta$ species. For binding experiments, A$\beta$ was incubated for not more than 1 h in the respective aggregation buffer (instead of dilution in the neuronal culture medium) on neurons to minimize reorganization. Here, N-terminal biotinylation affected neither the morphology nor the size of A$\beta$ aggregates, as exemplified by PL1 (Figure S6A of the Supporting Information). Binding was restricted to prefibrillar aggregates and mature neurons (DIV21). PL1, PL2, and PFB bound dose-dependently (Figure S6 of the Supporting Information) in a punctate pattern in contrast to Mono or FB (Figure 3). Furthermore, binding was not observed in young neurons [DIV7 (Figure S6E of the Supporting Information)].

Impairment of hippocampal neurotransmission was assessed by brief A$\beta$ incubations in aCSF within 30 min before reorganization was observed (Figure 2F). Field excitatory


dx.doi.org/10.1021/bi3016444 | Biochemistry 2013, 52, 1466–1476

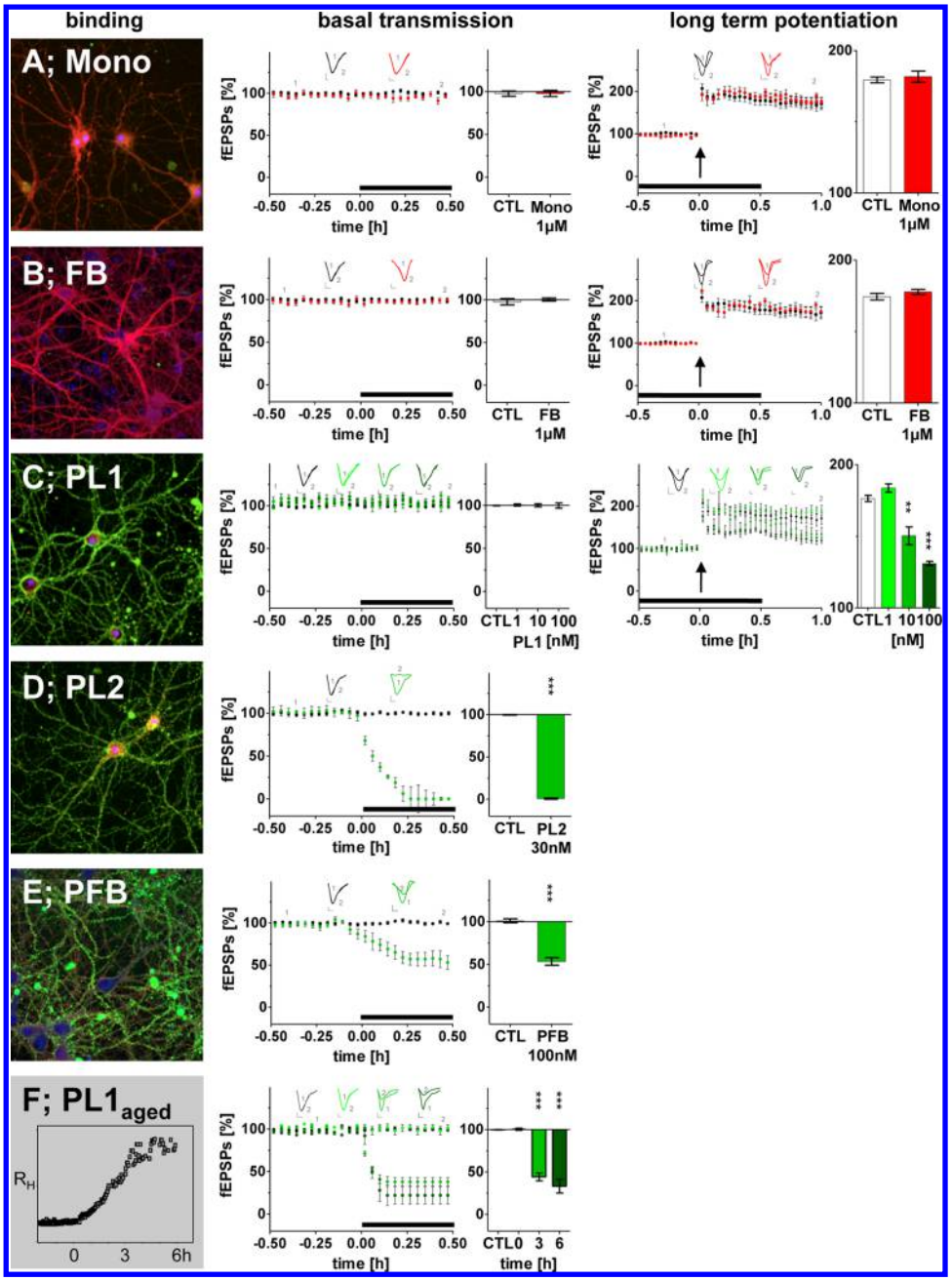


**Figure 3.** Soluble A$\beta$ aggregates differentially bound to mature hippocampal neurons and affected neurotransmission by different mechanisms. Mono (A) and FB (B) showed no binding, in contrast to the punctate binding of the prefibrillar preparations [biotinyl-A$\beta$ stained with Streptavidin-AF488 (green)]. AMPAR-dependent fEPSPs were recorded in the CA1 region of hippocampal rat slices for 30 min, followed by administration of freshly diluted A$\beta$ preparations. If basal transmission was not affected by the respective A$\beta$ assemblies, LTP was induced by HFS (100 Hz, 1 s). Individual fEPSPs are shown before (1) and after (2) A$\beta$ application (horizontal bar). Mono and FB had no effect on basal transmission or LTP (A and B, 1 $\mu$M). PL1 had no effect on synaptic transmission up to 100 nM. (C) LTP was reduced by PL1 dose-dependently, with the maximal effect occurring at 100 nM. (D) PL2 completely inhibited synaptic transmission at 30 nM. (E) PFB significantly inhibited synaptic transmission at 100 nM. Aging of PL1 in aCSF caused an inhibition of basal transmission depending on the preincubation time in aCSF [10 nM (E)]. The fEPSP amplitudes are given in percent of baseline (mean ± standard error of the mean of at least five independent experiments).

postsynaptic potentials (fEPSPs) were analyzed before [basal neurotransmission (BNT)] and after induction of long-term potentiation (LTP) by high-frequency stimuli (100 Hz, 1 s) in the presence of A$\beta$ (Figure 3). To avoid buffer-related artifacts, all A$\beta$ preparations were compared to control measurements in the respective A$\beta$-free aggregation buffers (%CTL). FB and Mono (both up to 1 $\mu$M) affected neither BNT nor LTP (Figure 3A,B). PL1 did not affect BNT at 100 nM (CTL, 100 ± 1; PL1, 100 ± 1, n.s.); however, it did inhibit LTP dose-dependently (Figure 3C; CTL, 176 ± 2; PL1, 184 ± 3 at 1 nM, 150 ± 6** at 10 nM, and 131 ± 2*** at 100 nM). In contrast, PL2 (30 nM) inhibited BNT completely within 15 min (Figure 3D; CTL, 100 ± 1; PL2, 0 ± 0***). Thus, induction of LTP could not be addressed. Similarly, PFB significantly inhibited BNT at 100 nM (Figure 3E; CTL, 100 ± 1; PFB, 56 ± 2***). Remarkably, preincubation of PL1 in aCSF for 3 or 6 h prior to the experiment ($PL1_{aged}$) led to an inhibition of BNT, which increased with time of aging (Figure 3F; 100 ± 1 at 0 h, 44 ±


dx.doi.org/10.1021/bi3016444 | *Biochemistry* 2013, 52, 1466−1476

5*** at 3 h, and 33 ± 8*** at 6 h). Thus, the conversion of spheroidal PL1 to protofibrillar/fibrillar $PL1_{aged}$ was paralleled by a switch from impaired LTP to BNT. In summary, neither monomeric nor fibrillar Aβ bound to neurons or affected neurotransmission. In contrast, the prefibrillar Aβ preparations bound to neurons and affected two different modalities of hippocampal neurotransmission, i.e., either BNT (PL2, PFB, and $PL1_{aged}$) or LTP (PL1).

## DISCUSSION

Soluble Aβ aggregates are considered to cause synaptotoxicity and cognitive decline in AD.[6,30] In the past two decades, cell-derived and synthetic Aβ species have been extensively characterized. This has led to the description of a variety of Aβ species claiming distinct entities and pathogenic modalities, resulting in a controversial debate about the pathophysiological relevance of a distinct Aβ aggregate in AD.[7]

The methods generally applied for characterization of endogenous or synthetic Aβ do not resolve this debate. Nevertheless, the accessible methods allow for comparison of synthetic spheroidal and protofibrillar Aβ aggregates and their associated bioactivity, which has not been investigated intensively to the best of our knowledge. Here, synthetic Aβ preparations were differentiated in AFM followed by semi-automated particle recognition, improving the statistical accuracy and precision of absolute height. AF4-MALS and DLS were applied to assess the MW distribution, homogeneity, and stability in solution, which is crucial for attributing an observed bioactivity to a predominant Aβ aggregate.

**Aβ Aggregate Preparations.** To initiate assembly of Aβ from the monomeric state, NaOH[12] instead of DMSO[31] was applied to obtain a seedless Aβ stock solution, which resulted in a higher yield of soluble Aβ aggregates. Because of the instant aggregation of Aβ42, Aβ40 was used as monomeric control. Mono remained predominantly monomeric as shown by DLS, AF4-MALS, and AFM. In contrast, freshly dissolved Aβ42, frequently used as a monomer control,[32,33] revealed rapid aggregation and thus was considered as a mixture of nascent Aβ assemblies comprising LMWO and larger aggregates as described by others.[14,19,34] PL1 appeared to be similar to ADDL, revealing spheroidal particles with a height of 6 nm and an elution profile in SEC (Figure S4 of the Supporting Information) as described by others.[31,35] The observed AFM dimensions of PL1 were in line with the MW distribution in AF4-MALS, if spheroidal to disk-shaped Aβ assemblies are considered.[11,35] In AF4-MALS, PL1 appeared as continuously distributed Aβ assemblies with a MW of 73 kDa at peak and thus smaller than ADDL analyzed by SEC-MALS (250−500 kDa at peak[9,32]). This discrepancy might relate to the improved resolution of AF4 compared to that of SEC, illustrated by the separation of PL1 and PFB (644 kDa at peak) in AF4-MALS. Notably, the Sephadex-75 column focuses aggregates >60 kDa in the void volume as described for protofibrils and ADDL (Figure S4 of the Supporting Information[9,20,36]). PL2 revealed a bimodal height distribution via AFM with spherical Aβ assemblies of 2 and 6 nm, with the latter being slightly elongated (38 nm), potentially relating to protofibrillar precursors. Comparable results have been described for early disk-shaped Aβ assemblies obtained via PBS at 4 °C in single-touch AFM experiments with a height of 2−3 nm and a diameter of 10−15 nm. These aggregates are described as penta- to hexameric Aβ42, coexisting with multiple layers of these aggregates, which might reflect PL2-P2.[11,19] Characterization of PFB and FB confirmed published data revealing cross β-sheet containing curvilinear structures of >150 kDa and >1 MDa and 50 nm and several micrometers in length, respectively.[10,19,36,37]

**Metastability of Aβ Aggregates.** The cytotoxic potency of Aβ aggregates is frequently determined by the sequential characterization of Aβ aggregate morphology and the biological experiment. The characterization is *prefacto*, and attributing an observed effect to a certain species requires stability under the conditions of the biological experiment.[8] Here we showed that *prefacto*-characterized Aβ aggregates are stable, but only if kept in their original environment. Indeed, a change in the ionic environment provoked reorganization of metastable monomeric Aβ40 and PL1 aggregates, indicating that applied buffer conditions are highly relevant for not only ab initio aggregation[8,10,19,38] but also in situ, if bioactivity of preformed Aβ aggregates is addressed. The provoked aggregation of Mono or PL1 to protofibrillar and fibrillar assemblies by dilution in neurobasal medium most likely explains why comparable neurotoxicity was observed after 48 h. Similarly, in situ Aβ aggregation has been shown to be prerequisite for neurotoxicity[39,40] and might be related to a unique cytotoxic potential for each individual species on the pathway to fibrils.[15,41] The rapid rearrangement in combination with long incubation times challenges the experimentally determined cytotoxic potentials, because structural characterization and the biological experiment are temporally incoherent. To summarize, our setup revealed that all aggregation protocols generated Aβ aggregates with favored morphology and MW, but no distinct Aβ species. Notably, Aβ42 aggregation in PBS, DMEM, or Ham's F12 resulted in different predominant Aβ aggregates. Thus, slight changes in aggregation protocols result in Aβ preparations with variable aggregate compositions and might contribute to controversial results, as exemplified by the interaction of Aβ with the prion protein.[32,33,42] Indeed, these examples all used different aggregation conditions while referring to ADDL, originally described by Lambert et al.[31] All Aβ aggregates are metastable, and subtle changes in the ionic environment led to reorganization, both *prefacto* and in situ. The importance of the applied ionic environment has generally been underestimated and has to be critically reviewed to allow for comparison of biological effects.

**Different Soluble Aβ Aggregates Mediate Synaptotoxicity by Different Mechanisms.** In contrast to neurotoxicity measurements, we chose neuronal binding and hippocampal neurotransmission as surrogate models to assess the bioactivity of a certain Aβ preparation. Both settings revealed short-term incubations, and aggregate reorganization was negligible. As described by others, Mono[9] and FB[43] did not bind. In contrast, prefibrillar aggregates (PL1, PL2, and PFB) demonstrated a punctate pattern of binding to mature neurons, as shown for ADDL[27,44−46] and PFB.[18] To test for relevance of Aβ aggregates on learning and memory, BNT and LTP were investigated separately.[31,47,48] BNT is dominated by the activation of AMPAR[28,49] in contrast to the induction of NMDAR-dependent LTP,[50−52] which requires activation of both AMPAR- and NMDAR-dependent pathways. For the induction of LTP, the high sodium conductivity of AMPAR allows for full depolarization of the synapse required for activation of NMDAR.[53,54] To attribute Aβ-related effects on NMDAR-dependent LTP, BNT must not be impaired and vice versa: if BNT is affected, NMDAR-independent pathways are involved. Thus, this setting was suitable for differentiation of

two different synaptotoxic modalities. However, because of the various possibilities for modulating AMPAR and NMDAR,[55] an impairment of BNT and LTP do not provide evidence of a distinct target of Aβ. Monomeric and fibrillar Aβ affected neither BNT nor LTP, supporting the concept that Aβ monomers and fibrils are virtually inactive.[18,56] Consistent with the binding experiments, all prefibrillar aggregates affected neurotransmission, although by different mechanisms. PL1 did not affect BNT but inhibited NMDAR-dependent LTP dose-dependently, as described for ADDL,[57,58] providing further evidence that PL1 and ADDL are equal in size, morphology, and bioactivity by all measures. In contrast to PL1, PL2 and PFB impaired BNT. These preparations rapidly inhibited BNT with nanomolar potency indicative of impaired AMPAR signaling. Similar data for this rapid onset of action on BNT have been obtained for small nascent ThioT-positive Aβ aggregates[15] and protofibrillar Aβ preparations.[37] Although a conformational change in Aβ aggregates upon binding to the neuronal matrix cannot be ruled out, it is tempting to speculate that PL2 and PFB are intermediates of the same aggregation pathway and share similar conformational elements. This hypothesis is based on their joint inhibitory effect on AMPAR-dominated BNT and their morphology in AFM, resembling hexameric Aβ and multiples hereof.[11,19] Although this hypothesis needs further experimental validation, it seems to be an attractive model for explaining why both preparations inhibited BNT. In addition, the provoked conversion of PL1 to protofibrillar and fibrillar aggregates, which was paralleled by a time-dependent suppression of BNT, indicates a change in the modality of synaptic suppression and thus stresses both the importance of addressing the metastability and the unaffected BNT, before LTP induction. Especially the latter has been discussed recently for the controversial debate about the interaction of ADDL with the prion protein[32,42] and may explain why Hartley et al.[56] observed LTP inhibition with cross-linked Aβ protofibrils, without investigating BNT. Whether inhibition of AMPAR-dependent BNT or NMDAR-dependent LTP represents a distinct mechanism or a mixed effect remains to be investigated, because of the various possibilities of modulating negatively AMPAR and NMDAR. Nevertheless, ADDL (here PL1) has been reported to interact directly with mGluR5[59] or the prion protein,[32,42] which both critically affect NMDAR function[43,44,48,60,61] and thus provide a mechanistic model in line with our results for LTP inhibition by PL1. With regard to BNT, several studies described a direct inhibitory action of Aβ on AMPAR, which could be related to the observed effects, although the aggregation state or morphology was hardly characterized.[62−65]

A further mechanism, possibly affecting LTP and BNT, is based on the affinity of Aβ for the neuronal membrane. Indeed, because of its hydrophobicity, Aβ is able to interact with the lipid bilayer of the neuronal membrane. The consequence of such an interaction could influence the fluidity of the lipid bilayer,[66,67] change the properties of the membrane via insertion,[68] or promote the release of membrane lipids. This results in impaired lipid homeostasis[69] and can lead to the formation of amyloid pores, thus affecting plasma membrane integrity and conductivity.[70,71] It has been reported that monomeric Aβ, low-molecular weight aggregates, and oligomeric Aβ penetrate into the lipid bilayer, resulting in a thinning of the membrane[72] and an altered structure and fluidity.[73,74] In addition, it has been shown that Aβ tends to aggregate further upon binding to the lipid bilayer, because of surface charge and hydrophobicity.[75] Thus, the Aβ peptide promotes structural changes in the neuronal membrane and vice versa. Aβ aggregates have varying affinities for membrane lipids such as monosialoganglioside GM1, cholesterol, and sphingomyelin, which are predominant in lipid rafts. Given that the local environment of the membrane differs ultrastructurally for lipid rafts, postsynaptic densities and perisynaptic regions, as well as for the local environment of membrane-anchored receptor and structure proteins such as NMDAR, AMPAR, integrins, and PSD95,[76,77] one could assume that the different Aβ aggregate species interact both with membrane proteins and with the membrane itself. Because the receptor function is also dependent on a defined structural environment, Aβ could trigger a concerted action on the membrane, receptors, and related structure and scaffolding proteins. The PL2 presented here might be involved in the AMPAR pathway; however, unspecific depolarization as a result of pore formation could also result in a decreased level of BNT. Nevertheless, PL1 interacts differently, either by direct interaction with the NMDAR pathway or by changing local membrane conditions resulting in the inhibition of NMDAR signaling.

Finally, various Aβ assemblies, derived from cells, transgenic tissue, or synthetic peptide, have been shown to impair cognition in vivo;[78] the fate of these assemblies within the brain could not be investigated previously.[7] Therefore, we aimed for a head-to-head comparison in vitro, where the difference in Aβ aggregate morphology and fate is accessible, and obtained different synaptotoxic modalities for different Aβ assemblies. Although the prefibrillar Aβ preparations were highly potent in impairing neurotransmission, they did not represent a single entity and were metastable, confounding a quantitative assessment of their unique cytotoxic potential. Our study reveals that Aβ aggregates do not represent distinct entities but rather equivocal distributions in morphology and MW. All assemblies are only metastable, and thus, each manipulation for assessing their specific activity in biological paradigms should avoid prolonged incubation in different environments. This minimizes confounding factors and allows us to address the unique cytotoxic potential of certain Aβ aggregates. Furthermore, our study shows that different Aβ aggregates are relevant in AD, because both spheroidal and protofibrillar Aβ aggregates inhibit hippocampal neurotransmission by different modalities. This challenges the therapeutical approach to target a specific "toxic" Aβ assembly because Aβ aggregates reveal synaptotoxicity by various modalities.

## ■ ASSOCIATED CONTENT

### Supporting Information

AFM particle analysis (Figure S1), Aβ solubilization (Figure S2), AFM oversegmentation (Figure S3), Aβ in SDS−PAGE and SEC (Figure S4), Aβ in TEM, Thio-T, and A11 Dotblot (Figure S5), and Aβ binding to hippocampal cultures (Figure S6). This material is available free of charge via the Internet at http://pubs.acs.org.

## ■ AUTHOR INFORMATION

### Corresponding Author

*Telephone: +49 176 31446383. E-mail: jensmoreth@gmail.com.

### Author Contributions

J.M. designed the study, performed the biochemical, biophysical, and biological experiments, maintained the primary

neuronal culture, analyzed the data, and wrote the paper. K.S.K. performed the electrophysiological experiments. D.S. maintained the primary neuronal culture and performed the toxicity experiments. C.S., C.A.F.v.A., B.H., and H.R. supported in writing the paper. L.K. coordinated the study, analyzed the data, and wrote the paper.

### Funding

This work was funded by Boehringer Ingelheim Pharma GmBH & Co. KG (CNS Department) and the University of Ulm (Department of Neurology).

### Notes

The authors declare no competing financial interest.

## ■ ACKNOWLEDGMENTS

We thank Andrew Doig, Kelly Allers, Scott Hobson, Owen Scudamore and Martin Scudamore for carefully reviewing the manuscript.

## ■ ABBREVIATIONS

aCSF, artificial cerebrospinal fluid; ADDL, Alzheimer-derived diffusible ligand; AF4, asymmetrical flow field-flow fractionation; AFM, atomic force microscopy; AMPAR, AMPA receptor; A$\beta$, amyloid $\beta$; A$\beta$O, amyloid $\beta$ oligomer; BNT, basal neurotransmission; CaMK, $Ca^{2+}$ calmodulin kinase; DIV, days in vitro; DLS, dynamic light scattering; FB, fibril preparation; fEPSP, field excitatory postsynaptic potential; HFIP, hexafluoro-2-propanol; HFS, high-frequency stimulation; LMWO, low-molecular weight oligomer; LTP, long-term potentiation; MALS, multiangle light scattering; Mono, monomer preparation; MTT, dimethylthiazoldiphenyltetrazolium bromide; MW, molecular weight; NMDAR, NMDA receptor; PAGE, polyacrylamide gel electrophoresis; PES, polyethersulfon; PFB, protofibril preparation; PL1/PL2, oligomer aggregate 1/2 preparation; $R_H$, hydrodynamic radius; SDS, sodium dodecyl sulfate; TEM, transmission electron microscopy.

## ■ REFERENCES

(1) Selkoe, D. J. (2001) Alzheimer's Disease: Genes, Proteins, and Therapy. *Physiol. Rev. 81*, 741−766.

(2) Broersen, K., Rousseau, F., and Schymkowitz, J. (2010) The culprit behind amyloid $\beta$ peptide related neurotoxicity in Alzheimer's disease: Oligomer size or conformation? *Alzheimer's Res. Ther. 2*, 12.

(3) Haass, C. (2004) Take five: BACE and the $\gamma$-secretase quartet conduct Alzheimer's amyloid $\beta$-peptide generation. *EMBO J. 23*, 483−488.

(4) Mc Donald, J. M., Savva, G. M., Brayne, C., Welzel, A. T., Forster, G., Shankar, G. M., Selkoe, D. J., Ince, P. G., and Walsh, D. M. (2010) The presence of sodium dodecyl sulphate-stable A dimers is strongly associated with Alzheimer-type dementia. *Brain 133*, 1328−1341 (on behalf of the Medical Research Council Cognitive Function and Ageing Study).

(5) Terry, R. D. (2006) Alzheimer's Disease and the Aging Brain. *Journal of Geriatric Psychiatry and Neurology 19*, 125−128.

(6) Walsh, D. M., and Selkoe, D. J. (2007) A$\beta$ oligomers: A decade of discovery. *J. Neurochem. 101*, 1172−1184.

(7) Benilova, I., Karran, E., and De Strooper, B. (2012) The toxic A$\beta$ oligomer and Alzheimer's disease: An emperor in need of clothes. *Nat. Neurosci. 15*, 349−357.

(8) Bitan, G., Fradinger, E. A., Spring, S. M., and Teplow, D. B. (2005) Neurotoxic protein oligomers: What you see is not always what you get. *Amyloid 12*, 88−95.

(9) Hepler, R. W., Grimm, K. M., Nahas, D. D., Breese, R., Dodson, E. C., Acton, P., Keller, P. M., Yeager, M., Wang, H., Shughrue, P., Kinney, G., and Joyce, J. G. (2006) Solution State Characterization of Amyloid $\beta$-Derived Diffusible Ligands. *Biochemistry 45*, 15157−15167.

(10) Stine, W. B. (2002) In Vitro Characterization of Conditions for Amyloid-$\beta$ Peptide Oligomerization and Fibrillogenesis. *J. Biol. Chem. 278*, 11612−11622.

(11) Mastrangelo, I. A., Ahmed, M., Sato, T., Liu, W., Wang, C., Hough, P., and Smith, S. O. (2006) High-resolution Atomic Force Microscopy of Soluble A$\beta$42 Oligomers. *J. Mol. Biol. 358*, 106−119.

(12) Rahimi, F., Shanmugam, A., and Bitan, G. (2008) Structure-function relationships of pre-fibrillar protein assemblies in Alzheimer's disease and related disorders. *Curr. Alzheimer Res. 5*, 319−341.

(13) Fezoui, Y., Hartley, D. M., Harper, J. D., Khurana, R., Walsh, D. M., Condron, M. M., Selkoe, D. J., Lansbury, P. T., Fink, A. L., and Teplow, D. B. (2000) An improved method of preparing the amyloid $\beta$-protein for fibrillogenesis and neurotoxicity experiments. *Amyloid 7*, 166−178.

(14) Bitan, G. (2002) Amyloid $\beta$-protein (A$\beta$) assembly: A$\beta$40 and A$\beta$42 oligomerize through distinct pathways. *Proc. Natl. Acad. Sci. U.S.A. 100*, 330−335.

(15) Kuperstein, I., Broersen, K., Benilova, I., Rozenski, J., Jonckheere, W., Debulpaep, M., Vandersteen, A., Segers-Nolten, I., Van Der Werf, K., Subramaniam, V., Braeken, D., Callewaert, G., Bartic, C., D'Hooge, R., Martins, I. C., Rousseau, F., Schymkowitz, J., and De Strooper, B. (2010) Neurotoxicity of Alzheimer's disease A$\beta$ peptides is induced by small changes in the A$\beta$42 to A$\beta$40 ratio. *EMBO J. 29*, 3408−3420.

(16) Necula, M., Kayed, R., Milton, S., and Glabe, C. G. (2007) Small Molecule Inhibitors of Aggregation Indicate That Amyloid $\beta$ Oligomerization and Fibrillization Pathways Are Independent and Distinct. *J. Biol. Chem. 282*, 10311−10324.

(17) Roychaudhuri, R., Yang, M., Hoshi, M. M., and Teplow, D. B. (2009) Amyloid $\beta$-protein assembly and Alzheimer disease. *J. Biol. Chem. 284*, 4749−4753.

(18) Martins, I. C., Kuperstein, I., Wilkinson, H., Maes, E., Vanbrabant, M., Jonckheere, W., Van Gelder, P., Hartmann, D., D'Hooge, R., De Strooper, B., Schymkowitz, J., and Rousseau, F. (2007) Lipids revert inert A$\beta$ amyloid fibrils to neurotoxic protofibrils that affect learning in mice. *EMBO J. 27*, 224−233.

(19) Ahmed, M., Davis, J., Aucoin, D., Sato, T., Ahuja, S., Aimoto, S., Elliott, J. I., Van Nostrand, W. E., and Smith, S. O. (2010) Structural conversion of neurotoxic amyloid-$\beta$(1−42) oligomers to fibrils. *Nat. Struct. Mol. Biol. 17*, 561−567.

(20) O'Nuallain, B., Freir, D. B., Nicoll, A. J., Risse, E., Ferguson, N., Herron, C. E., Collinge, J., and Walsh, D. M. (2010) Amyloid $\beta$-Protein Dimers Rapidly Form Stable Synaptotoxic Protofibrils. *J. Neurosci. 30*, 14411−14419.

(21) Haass, C. (2010) Initiation and propagation of neurodegeneration. *Nat. Med. 16*, 1201−1204.

(22) Lomakin, A., and Teplow, D. B. (2006) Quasielastic light scattering study of amyloid $\beta$-protein fibril formation. *Protein Pept. Lett. 13*, 247−254.

(23) Zattoni, A., Rambaldi, D. C., Reschiglian, P., Melucci, M., Krol, S., Garcia, A. M. C., Sanz-Medel, A., Roessner, D., and Johann, C. (2009) Asymmetrical flow field-flow fractionation with multi-angle light scattering detection for the analysis of structured nanoparticles. *J. Chromatogr., A 1216*, 9106−9112.

(24) Fraunhofer, W., and Winter, G. (2004) The use of asymmetrical flow field-flow fractionation in pharmaceutics and biopharmaceutics. *Eur. J. Pharm. Biopharm. 58*, 369−383.

(25) Cremona, M., Mauricio, M., Scavarda Do Carmo, L. C., Prioli, R., Nunes, V., Zanette, S., Caride, A., and Albuquerque, M. (2000) Grain size distribution analysis in polycrystalline LiF thin films by mathematical morphology techniques on AFM images and X-ray diffraction data. *J. Microsc. 197*, 260−267.

(26) Brewer, G. J., Torricelli, J. R., Evege, E. K., and Price, P. J. (1993) Optimized survival of hippocampal neurons in B27-supplemented neurobasal, a new serum-free medium combination. *J. Neurosci. Res. 35*, 567−576.

(27) Lacor, P. N. (2004) Synaptic Targeting by Alzheimer's-Related Amyloid Oligomers. *J. Neurosci. 24*, 10191−10200.
(28) Kroker, K. S., Rosenbrock, H., and Rast, G. (2011) A multi-slice recording system for stable late phase hippocampal long-term potentiation experiments. *J. Neurosci. Methods 194*, 394−401.
(29) Collingridge, G. L., Kehl, S. J., Loo, R., and McLennan, H. (1983) Effects of kainic and other amino acids on synaptic excitation in rat hippocampal slices: 1. Extracellular analysis. *Exp. Brain Res. 52*, 170−178.
(30) Hardy, J., and Selkoe, D. J. (2002) The amyloid hypothesis of Alzheimer's disease: Progress and problems on the road to therapeutics. *Science 297*, 353−356.
(31) Lambert, M. P., Barlow, A. K., Chromy, B. A., Edwards, C., Freed, R., Liosatos, M., Morgan, T. E., Rozovsky, I., Trommer, B., Viola, K. L., Wals, P., Zhang, C., Finch, C. E., Krafft, G. A., and Klein, W. L. (1998) Diffusible, nonfibrillar ligands derived from Aβ1−42 are potent central nervous system neurotoxins. *Proc. Natl. Acad. Sci. U.S.A. 95*, 6448−6453.
(32) Laurén, J., Gimbel, D. A., Nygaard, H. B., Gilbert, J. W., and Strittmatter, S. M. (2009) Cellular prion protein mediates impairment of synaptic plasticity by amyloid-β oligomers. *Nature 457*, 1128−1132.
(33) Balducci, C., Beeg, M., Stravalaci, M., Bastone, A., Sclip, A., Biasini, E., Tapella, L., Colombo, L., Manzoni, C., Borsello, T., Chiesa, R., Gobbi, M., Salmona, M., and Forloni, G. (2010) Synthetic amyloid-β oligomers impair long-term memory independently of cellular prion protein. *Proc. Natl. Acad. Sci. U.S.A. 107*, 2295−2300.
(34) Bitan, G., Vollers, S. S., and Teplow, D. B. (2003) Elucidation of primary structure elements controlling early amyloid β-protein oligomerization. *J. Biol. Chem. 278*, 34882−34889.
(35) Chromy, B. A., Nowak, R. J., Lambert, M. P., Viola, K. L., Chang, L., Velasco, P. T., Jones, B. W., Fernandez, S. J., Lacor, P. N., Horowitz, P., Finch, C. E., Krafft, G. A., and Klein, W. L. (2003) Self-Assembly of Aβ 1−42 into Globular Neurotoxins. *Biochemistry 42*, 12749−12760.
(36) Walsh, D. M., Hartley, D. M., Kusumoto, Y., Fezoui, Y., Condron, M. M., Lomakin, A., Benedek, G. B., Selkoe, D. J., and Teplow, D. B. (1999) Amyloid β-protein fibrillogenesis. Structure and biological activity of protofibrillar intermediates. *J. Biol. Chem. 274*, 25945−25952.
(37) Hartley, D. M., Walsh, D. M., Ye, C. P., Diehl, T., Vasquez, S., Vassilev, P. M., Teplow, D. B., and Selkoe, D. J. (1999) Protofibrillar intermediates of amyloid β-protein induce acute electrophysiological changes and progressive neurotoxicity in cortical neurons. *J. Neurosci. 19*, 8876−8884.
(38) Itkin, A., Dupres, V., Dufrêne, Y. F., Bechinger, B., Ruysschaert, J.-M., and Raussens, V. (2011) Calcium Ions Promote Formation of Amyloid β-Peptide (1−40) Oligomers Causally Implicated in Neuronal Toxicity of Alzheimer's Disease. *PLoS One 6*, e18250.
(39) Wogulis, M. (2005) Nucleation-Dependent Polymerization Is an Essential Component of Amyloid-Mediated Neuronal Cell Death. *J. Neurosci. 25*, 1071−1080.
(40) Jan, A., Adolfsson, O., Allaman, I., Buccarello, A. L., Magistretti, P. J., Pfeifer, A., Muhs, A., and Lashuel, H. A. (2011) Aβ42 neurotoxicity is mediated by ongoing nucleated polymerization process rather than by discrete Aβ42 species. *J. Biol. Chem. 286*, 8585−8596.
(41) Ono, K., Condron, M. M., and Teplow, D. B. (2009) Structure-neurotoxicity relationships of amyloid β-protein oligomers. *Proc. Natl. Acad. Sci. U.S.A. 106*, 14745−14750.
(42) Kessels, H. W., Nguyen, L. N., Nabavi, S., and Malinow, R. (2010) The prion protein as a receptor for amyloid-β. *Nature 466*, E3−E4.
(43) De Felice, F. G., Wu, D., Lambert, M. P., Fernandez, S. J., Velasco, P. T., Lacor, P. N., Bigio, E. H., Jerecic, J., Acton, P. J., Shughrue, P. J., Chen-Dodson, E., Kinney, G. G., and Klein, W. L. (2008) Alzheimer's disease-type neuronal tau hyperphosphorylation induced by Aβ oligomers. *Neurobiol. Aging 29*, 1334−1347.
(44) Lacor, P. N., Buniel, M. C., Furlow, P. W., Sanz Clemente, A., Velasco, P. T., Wood, M., Viola, K. L., and Klein, W. L. (2007) A Oligomer-Induced Aberrations in Synapse Composition, Shape, and Density Provide a Molecular Basis for Loss of Connectivity in Alzheimer's Disease. *J. Neurosci. 27*, 796−807.
(45) Deshpande, A. (2006) Different Conformations of Amyloid β Induce Neurotoxicity by Distinct Mechanisms in Human Cortical Neurons. *J. Neurosci. 26*, 6011−6018.
(46) Shughrue, P. J., Acton, P. J., Breese, R. S., Zhao, W. Q., Chen-Dodson, E., Hepler, R. W., Wolfe, A. L., Matthews, M., Heidecker, G. J., Joyce, J. G., Villarreal, S. A., and Kinney, G. G. (2010) Anti-ADDL antibodies differentially block oligomer binding to hippocampal neurons. *Neurobiol. Aging 31*, 189−202.
(47) Walsh, D. M., Klyubin, I., Fadeeva, J. V., Cullen, W. K., Anwyl, R., Wolfe, M. S., Rowan, M. J., and Selkoe, D. J. (2002) Naturally secreted oligomers of amyloid β protein potently inhibit hippocampal long-term potentiation in vivo. *Nature 416*, 535−539.
(48) Wang, Q. (2004) Block of Long-Term Potentiation by Naturally Secreted and Synthetic Amyloid β-Peptide in Hippocampal Slices Is Mediated via Activation of the Kinases c-Jun N-Terminal Kinase, Cyclin-Dependent Kinase 5, and p38 Mitogen-Activated Protein Kinase as well as Metabotropic Glutamate Receptor Type 5. *J. Neurosci. 24*, 3370−3378.
(49) Dingledine, R., Borges, K., Bowie, D., and Traynelis, S. F. (1999) The glutamate receptor ion channels. *Pharmacol. Rev. 51*, 7−61.
(50) Harris, E. W., Ganong, A. H., and Cotman, C. W. (1984) Long-term potentiation in the hippocampus involves activation of N-methyl-D-aspartate receptors. *Brain Res. 323*, 132−137.
(51) Collingridge, G. L. (2003) The induction of N-methyl-D-aspartate receptor-dependent long-term potentiation. *Philos. Trans. R. Soc. B 358*, 635−641.
(52) Kroker, K. S., Rast, G., and Rosenbrock, H. (2011) Differential effect of the mGlu5 receptor positive allosteric modulator ADX-47273 on early and late hippocampal LTP. *Neuropharmacology 61*, 707−714.
(53) Muller, D., Joly, M., and Lynch, G. (1988) Contributions of quisqualate and NMDA receptors to the induction and expression of LTP. *Science 242*, 1694−1697.
(54) Watt, A. J., Sjöström, P. J., Häusser, M., Nelson, S. B., and Turrigiano, G. G. (2004) A proportional but slower NMDA potentiation follows AMPA potentiation in LTP. *Nat. Neurosci. 7*, 518−524.
(55) Yamin, G. (2009) NMDA receptor-dependent signaling pathways that underlie amyloid β-protein disruption of LTP in the hippocampus. *J. Neurosci. Res. 87*, 1729−1736.
(56) Hartley, D. M., Zhao, C., Speier, A. C., Woodard, G. A., Li, S., Li, Z., and Walz, T. (2008) Transglutaminase induces protofibril-like amyloid β-protein assemblies that are protease-resistant and inhibit long-term potentiation. *J. Biol. Chem. 283*, 16790−16800.
(57) Wang, H.-W., Pasternak, J. F., Kuo, H., Ristic, H., Lambert, M. P., Chromy, B., Viola, K. L., Klein, W. L., Stine, W. B., Krafft, G. A., and Trommer, B. L. (2002) Soluble oligomers of β amyloid (1−42) inhibit long-term potentiation but not long-term depression in rat dentate gyrus. *Brain Res. 924*, 133−140.
(58) Viola, K. L., Velasco, P. T., and Klein, W. L. (2008) Why Alzheimer's is a disease of memory: The attack on synapses by Aβ oligomers (ADDLs). *J. Nutr., Health Aging 12*, 51S−7S.
(59) Renner, M., Lacor, P. N., Velasco, P. T., Xu, J., Contractor, A., Klein, W. L., and Triller, A. (2010) Deleterious Effects of Amyloid β Oligomers Acting as an Extracellular Scaffold for mGluR5. *Neuron 66*, 739−754.
(60) Collett, V. J., and Collingridge, G. L. (2004) Interactions between NMDA receptors and mGlu5 receptors expressed in HEK293 cells. *Br. J. Pharmacol. 142*, 991−1001.
(61) Khosravani, H., Zhang, Y., Tsutsui, S., Hameed, S., Altier, C., Hamid, J., Chen, L., Villemaire, M., Ali, Z., Jirik, F. R., and Zamponi, G. W. (2008) Prion protein attenuates excitotoxicity by inhibiting NMDA receptors. *J. Cell Biol. 181*, 551−565.
(62) Roselli, F. (2005) Soluble β-Amyloid1−40 Induces NMDA-Dependent Degradation of Postsynaptic Density-95 at Glutamatergic Synapses. *J. Neurosci. 25*, 11061−11070.

(63) Hsieh, H., Boehm, J., Sato, C., Iwatsubo, T., Tomita, T., Sisodia, S., and Malinow, R. (2006) AMPAR Removal Underlies Aβ-Induced Synaptic Depression and Dendritic Spine Loss. *Neuron 52*, 831−843.
(64) Parameshwaran, K., Sims, C., Kanju, P., Vaithianathan, T., Shonesy, B. C., Dhanasekaran, M., Bahr, B. A., and Suppiramaniam, V. (2007) Amyloid β-peptide Aβ1−42 but not Aβ1−40 attenuates synaptic AMPA receptor function. *Synapse 61*, 367−374.
(65) Gu, Z., Liu, W., and Yan, Z. (2009) β-Amyloid impairs AMPA receptor trafficking and function by reducing $Ca^{2+}$/calmodulin-dependent protein kinase II synaptic distribution. *J. Biol. Chem. 284*, 10639−10649.
(66) Mason, R. P., Jacob, R. F., Walter, M. F., Mason, P. E., Avdulov, N. A., Chochina, S. V., Igbavboa, U., and Wood, W. G. (1999) Distribution and fluidizing action of soluble and aggregated amyloid β-peptide in rat synaptic plasma membranes. *J. Biol. Chem. 274*, 18801−18807.
(67) Kremer, J. J., Pallitto, M. M., Sklansky, D. J., and Murphy, R. M. (2000) Correlation of β-amyloid aggregate size and hydrophobicity with decreased bilayer fluidity of model membranes. *Biochemistry 39*, 10309−10318.
(68) Eckert, G. P., Cairns, N. J., Maras, A., Gattaz, W. F., and Muller, W. E. (2000) Cholesterol modulates the membrane-disordering effects of β-amyloid peptides in the hippocampus: Specific changes in Alzheimer's disease. *Dementia Geriatr. Cognit. Disord. 11*, 181−186.
(69) Michikawa, M., Gong, J. S., Fan, Q. W., Sawamura, N., and Yanagisawa, K. (2001) A novel action of Alzheimer's amyloid β-protein (Aβ): Oligomeric Aβ promotes lipid release. *J. Neurosci. 21*, 7226−7235.
(70) Kagan, B. L., Azimov, R., and Azimova, R. (2004) Amyloid Peptide Channels. *J. Membr. Biol. 202*, 1−10.
(71) Lashuel, H. A., and Lansbury, P. T. (2006) Are amyloid diseases caused by protein aggregates that mimic bacterial pore-forming toxins? *Q. Rev. Biophys. 39*, 167.
(72) Kayed, R., Sokolov, Y., Edmonds, B., McIntire, T. M., Milton, S. C., Hall, J. E., and Glabe, C. G. (2004) Permeabilization of lipid bilayers is a common conformation-dependent activity of soluble amyloid oligomers in protein misfolding diseases. *J. Biol. Chem. 279*, 46363−46366.
(73) Ashley, R. H., Harroun, T. A., Hauss, T., Breen, K. C., and Bradshaw, J. P. (2006) Autoinsertion of soluble oligomers of Alzheimer's Aβ(1−42) peptide into cholesterol-containing membranes is accompanied by relocation of the sterol towards the bilayer surface. *BMC Struct. Biol. 6*, 21.
(74) Subasinghe, S., Unabia, S., Barrow, C. J., Mok, S. S., Aguilar, M. I., and Small, D. H. (2003) Cholesterol is necessary both for the toxic effect of Aβ peptides on vascular smooth muscle cells and for Aβ binding to vascular smooth muscle cell membranes. *J. Neurochem. 84*, 471−479.
(75) Williams, T. L., and Serpell, L. C. (2011) Membrane and surface interactions of Alzheimer's Aβ peptide: Insights into the mechanism of cytotoxicity. *FEBS J. 278*, 3905−3917.
(76) Verdier, Y., Zarándi, M., and Penke, B. (2004) Amyloid β-peptide interactions with neuronal and glial cell plasma membrane: Binding sites and implications for Alzheimer's disease. *J. Pept. Sci. 10*, 229−248.
(77) Jurado, S., and Knafo, S. (2012) Microscale AMPAR reorganization and dynamics of the postsynaptic density. *J. Neurosci. 32*, 7103−7105.
(78) Reed, M. N., Hofmeister, J. J., Jungbauer, L., Welzel, A. T., Yu, C., Sherman, M. A., Lesné, S., LaDu, M. J., Walsh, D. M., Ashe, K. H., and Cleary, J. P. (2011) Cognitive effects of cell-derived and synthetically derived Aβ oligomers. *Neurobiol. Aging 32*, 1784−1794.